JCB Article

Localization of the AP-3 adaptor complex defines a novel endosomal exit site for lysosomal membrane proteins

Andrew A. Peden,[1] Viola Oorschot,[2] Boris A. Hesser,[1] Cary D. Austin,[1] Richard H. Scheller,[1] and Judith Klumperman[2]

[1]Genentech Inc., South San Francisco, CA 94080
[2]Cell Microscopy Center, Department of Cell Biology and Institute for Biomembranes, University Medical Center Utrecht, 3584CX Utrecht, Netherlands

The adaptor protein (AP) 3 adaptor complex has been implicated in the transport of lysosomal membrane proteins, but its precise site of action has remained controversial. Here, we show by immuno-electron microscopy that AP-3 is associated with budding profiles evolving from a tubular endosomal compartment that also exhibits budding profiles positive for AP-1. AP-3 colocalizes with clathrin, but to a lesser extent than does AP-1. The AP-3– and AP-1–bearing tubular compartments contain endocytosed transferrin, transferrin receptor, asialoglycoprotein receptor, and low amounts of the cation-independent mannose 6-phosphate receptor and the lysosome-associated membrane proteins (LAMPs) 1 and 2. Quantitative analysis revealed that of these distinct cargo proteins, only LAMP-1 and LAMP-2 are concentrated in the AP-3–positive membrane domains. Moreover, recycling of endocytosed LAMP-1 and CD63 back to the cell surface is greatly increased in AP-3–deficient cells. Based on these data, we propose that AP-3 defines a novel pathway by which lysosomal membrane proteins are transported from tubular sorting endosomes to lysosomes.

Introduction

Heterotetrameric adaptor complexes play a role in the selection of cargo molecules and vesicle budding. In mammalian cells, there are at least four adaptor protein (AP) complexes (AP-1 through AP-4), each of which mediates a distinct membrane trafficking step (Robinson and Bonifacino, 2001). Adaptor complexes consist of four subunits: two large subunits (the so-called β subunit and the more divergent γ/α/δ/ε subunit in AP-1/2/3/4, respectively), a medium subunit (μ), and a small subunit (σ). The structure of the adaptor complexes resembles that of a "Mickey Mouse" head, with the COOH-terminal domains of the two large subunits protruding like ears (Heuser and Keen, 1988).

Although the AP-3 adaptor complex was identified relatively recently, a considerable amount of functional information has already been acquired, thanks to the availability of naturally occurring mutants. Loss of functional AP-3 complex leads to defects in the function of lysosomes and lysosome-related organelles. The most obvious trafficking defect in AP-3–deficient cells is that integral lysosomal membrane proteins (also known as lysosomal glycoproteins), including lysosome-associated membrane proteins (LAMPs) 1 and 2, LIMP-2, CD63, and CD1, show increased trafficking via the plasma membrane (Dell'Angelica et al., 1999; Rous et al., 2002; Sugita et al., 2002). Nevertheless, their steady-state distribution is still mainly lysosomal. Mannose 6-phosphate receptor–based transport of soluble lysosomal enzymes and cycling of the transferrin receptor (TfR) between the plasma membrane and endosomes are independent of AP-3 function (Le Borgne et al., 1998; Dell'Angelica et al., 1999).

Despite the accumulating evidence implicating AP-3 in the intracellular transport of lysosomal membrane proteins, the transport step that is mediated by AP-3 has remained unclear. In yeast, like in mammalian cells, AP-3 deletion leads to the missorting of the vacuolar membrane proteins alkaline phosphate and Vam3p, but does not affect the trafficking of Vps10p, the receptor for the soluble hydrolase

The online version of this article includes supplemental material.

Address correspondence to J. Klumperman, Cell Microscopy Center, Department of Cell Biology, University Medical Center Utrecht, AZU RM G02.525, Heidelberglaan 100, 3584CX Utrecht, Netherlands. Tel.: 31-30-250-6550. Fax: 31-30-254-1797. email: j.klumperman@lab.azu.nl

Key words: AP-3 adaptor protein; TGN; endosomes; immuno-EM; clathrin

Abbreviations used in this paper: AP, adaptor protein; ASGPR, asialoglycoprotein receptor; CI-MPR, cation-independent mannose 6-phosphate receptor; EE, early endosome; LAMP, lysosome-associated membrane protein; NRK, normal rat kidney; Tf, transferrin; Tf-biotin, biotinylated transferrin; TfR, transferrin receptor.

carboxypeptidase Y (Cowles et al., 1997; Stepp et al., 1997). By contrast, yeast VPS mutants are still able to sort vacuolar membrane proteins to the vacuole. Hence, it was proposed that in yeast, AP-3 mediates a direct pathway for vacuolar membrane proteins from the TGN to the vacuole (Odorizzi et al., 1998). In mammalian cells, immunofluorescence localization experiments of the AP-3 complex have revealed concentrated staining in the perinuclear region, partially overlapping with markers of the TGN, but also significant staining out in the cell periphery, partially colocalizing with endocytic markers such as TfR (Simpson et al., 1996, 1997; Dell'Angelica et al., 1997, 1999). The degree of overlap with either TGN or endosomal markers varied considerably between these experiments. EM localization analyses also indicated a dual localization of the AP-3 complex on the TGN, as well as on endosomes (Simpson et al., 1996; Dell'Angelica et al., 1998).

At present, two (not mutually exclusive) models have been proposed to explain the role of the AP-3 complex in lysosomal membrane protein trafficking in mammalian cells (for review see Starcevic et al., 2002). In the first model, as in yeast, AP-3 is proposed to be responsible for recruiting lysosomal membrane proteins into a direct transport pathway from the TGN to endosomes/lysosomes. Lack of AP-3 function would then result in increased amounts of newly synthesized proteins traveling from the TGN via the constitutive pathway to the plasma membrane, from where it would be internalized by AP-2–dependent endocytosis and subsequently transported to the lysosomes. The second model proposes that AP-3 functions at an early endosomal compartment in which lysosomal membrane proteins must be segregated from other membrane proteins that recycle back to the plasma membrane. Lack of functional AP-3 would then lead to a buildup on the plasma membrane and in the recycling system.

The role of clathrin in AP-3 function has also remained controversial. Two isoforms of the AP-3 β subunit are known, the ubiquitous β3A and the neuro (endocrine)-specific β3B, both of which contain a clathrin consensus-binding motif (Dell'Angelica et al., 1998; ter Haar et al., 2000). Biochemical analyses have shown that AP-3 can bind and recruit clathrin in vitro onto synthetic liposomes (Dell'Angelica et al., 1998; Drake et al., 2000). However, unlike AP-1 and AP-2, the AP-3 complex is not enriched in purified clathrin-coated vesicles (Simpson et al., 1996; unpublished data), and genetic and biochemical evidence suggest that the AP-3 complex does not require clathrin for function in vivo (Vowels and Payne, 1998; Wettey et al., 2002). Moreover, AP-3–deficient mammalian cells were shown to be rescued almost as well by a β3A construct lacking the consensus clathrin-binding site as by the wild-type construct, suggesting that clathrin binding to the β3A subunit of the AP-3 is not required for AP-3 function (Peden et al., 2002). Immuno-colocalization analyses of clathrin and AP-3 have also produced conflicting results (Simpson et al., 1996; Dell'Angelica et al., 1998; Peden et al., 2002). Thus, whether or not clathrin is required for AP-3 function still remains unclear.

To address these key questions on AP-3 function, we have generated an mAb against the δ subunit of the AP-3 complex, and have used this antibody to localize AP-3 by immuno-EM. This approach offers the unique possibility of localizing AP-3 in direct comparison to lysosomal membrane proteins, as well as with other cargo and coat proteins, at a resolution sufficient to define small membrane microdomains involved in protein sorting. Our results provide evidence for the function of the AP-3 complex in the trafficking of lysosomal membrane proteins from endosomes, whereas no support for a role at the TGN was found. Unexpectedly, our data indicate that the endosomal AP-3 pathway arises from early endosome (EE)–associated tubules rather than the endosomal vacuole, implicating tubular endosomes also involved in protein recycling as an important intermediate station in lysosomal membrane protein traffic to the lysosomes.

Results

Generation of mAbs against the δ subunit of AP-3

To investigate the localization of the AP-3 adaptor complex, it was necessary to generate antibodies that are suitable for immuno-EM experiments. To this end, we immunized mice with a GST fusion protein containing the hinge region (aa 608–800) of the δ subunit, as this region is the most immunogenic (Fig. S1 A, available at http://www.jcb.org/cgi/content/full/jcb.200311064/DC1). After fusion, the supernatants from the resulting hybridomas were screened by ELISA. Then, Western blotting and immunofluorescence was performed on both control and *mocha* fibroblasts (δ deficient) to confirm their specificity. SA4, the monoclonal used in this work, did not yield a Western or immunofluorescence signal in the *mocha* extracts or cells, confirming that the antibody is specific for the δ subunit and does not cross react with any other proteins (Fig. S1, B and C). Moreover, the monoclonal gives the characteristic staining pattern for AP-3 of punctate spots throughout the cytoplasm (Fig. S1 C).

Immuno-EM localization of the AP-3 complex on EE-associated tubules

To investigate the localization of the AP-3 adaptor complex in subcellular detail, ultrathin cryosections were prepared from HepG2 and normal rat kidney (NRK) cells, and were immunogold labeled with the different anti-δ-subunit mAbs. Significant specific immunogold labeling was obtained with several anti-AP-3 monoclonals, but SA4 was selected for this work as it gave the highest labeling efficiency, especially in cells fixed only with formaldehyde. Although we obtained a similar staining pattern for AP-3 in both cell lines, we concentrated on HepG2 cells because they exhibited stronger staining.

First, we addressed whether AP-3 resides on the TGN and/or on endosome-associated membranes. The tubular membrane network within a distance of ~500 nm from the trans-most cisternae of a Golgi stack was considered as TGN (Geuze et al., 1985). These membranes are enriched in cation-independent mannose 6-phosphate receptor (CI-MPR; Fig. 1) and TGN46 (unpublished data), and show clathrin-coated and AP-1–coated buds at their cytoplasmic surface (Fig. 1 A) that mediate the exit of CI-MPR from the TGN to the endosomes (Klumperman et al., 1993; Doray et al.,

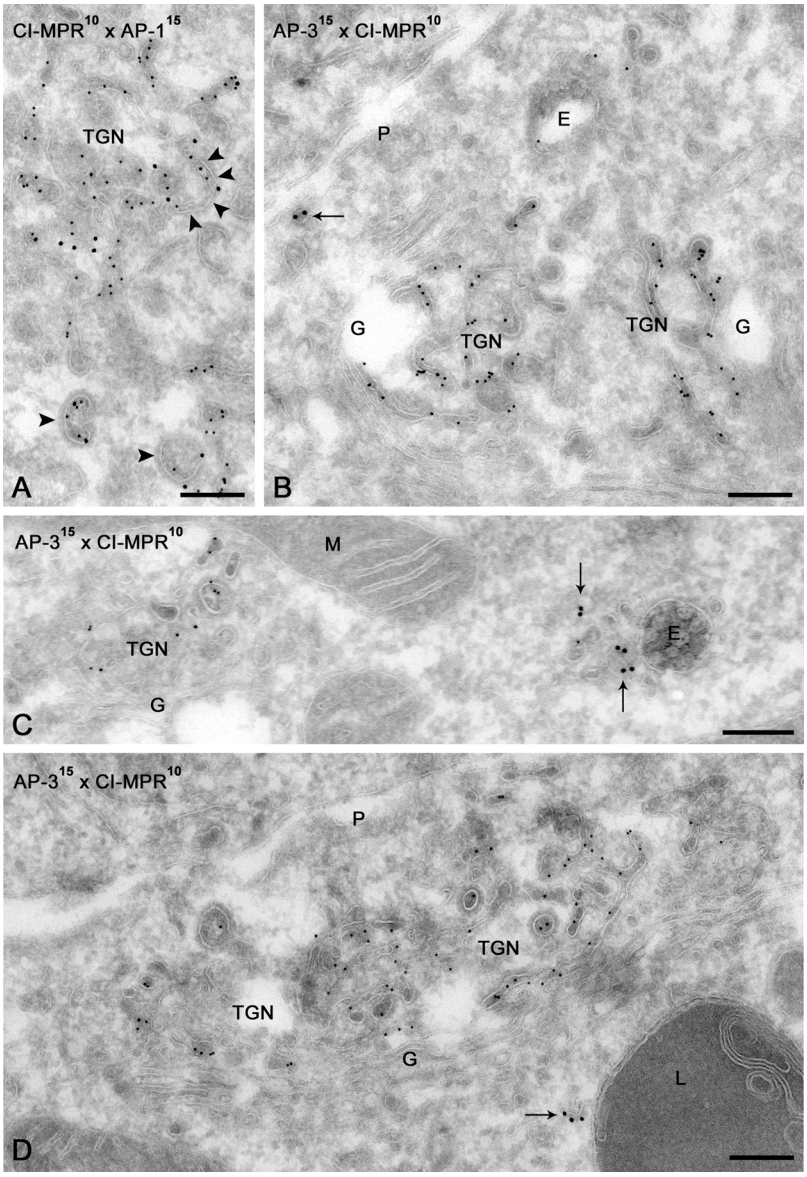

Figure 1. **AP-3 is not found in the TGN of HepG2 cells.** (A) In HepG2 cells, CI-MPR (10-nm gold) and AP-1 (15-nm gold) colocalize on membranes at the trans-side of the Golgi complex, indicating the position of the TGN. Some TGN membranes typically contain elongated stretches of clathrin (top row of arrowheads). The AP-1– and CI-MPR–labeled budding profiles in the TGN (bottom two arrowheads) are considerably wider than AP-3–labeled profiles (B–D, arrows). (B–D) AP-3 (15-nm gold) is not found on membranes in the TGN area, but on tubulo-vesicular profiles dispersed in the cytoplasm (B and D, arrows) or near endosomal vacuoles (C, arrows). E, endosome; G, Golgi complex; L, lysosome; M, mitochondrion; P, plasma membrane. Bars, 200 nm.

2002; Waguri et al., 2003). The average diameter of the CI-MPR and AP-1–positive buds on the TGN was 77 nm (n = 42). No significant AP-3 labeling was found in these TGN profiles (Fig. 1, B–D).

By contrast, AP-3 was present on highly convoluted tubules that were often found in close vicinity to endosomal vacuoles (Fig. 1 C and Fig. 2). On these tubules, AP-3 was associated with buds that were significantly smaller than those on the TGN, i.e., only 33 nm (n = 40; Fig. 2, A–E). The AP-3–positive tubules were reminiscent of the EE recycling tubules as described by others (Geuze et al., 1983; Marsh et al., 1986; Griffiths et al., 1989). Therefore, to assay the nature of these tubules, we performed colocalization experiments with internalized transferrin (Tf) and asialoglycoprotein receptor (ASGPR), both markers of the endosomal recycling pathway. After a 20-min internalization, biotinylated Tf (Tf-biotin) was found at the limiting membrane of EE vacuoles, as well as in the associated tubules (Fig. 2, A and B). By double labeling, we found AP-3–positive buds on the Tf-biotin–containing recycling tubules. Similar results were obtained when cells were double labeled for AP-3 and endogenous ASGPR (Fig. 2, C and D). Primary endocytic vesicles labeled with the endocytic tracer BSA-gold were consistently devoid of AP-3 label (unpublished data). AP-3–positive tubules also contained small amounts of CI-MPR (Fig. 2 E). The CI-MPR label was mostly found dispersed in the noncoated areas of the AP-3–positive tubules, but occasionally AP-3–negative buds were observed where CI-MPR was concentrated (Fig. 2, F and G; arrowheads). Together, these findings show that AP-3 resides on a tubular endosomal compartment that contains cargo proteins destined for recycling to the plasma membrane or the TGN.

AP-3 localizes to clathrin-coated membranes

Previous reports have not clearly resolved whether AP-3 uses clathrin as its structural scaffold in vivo. Therefore, we performed double labelings of AP-3 and clathrin (Fig. 3, A and B). AP-3 was found on membranes that were (Fig. 3 A) and were not (Fig. 3 B) labeled for clathrin. Moreover, AP-3–positive buds were also seen on tubules that displayed cloth-

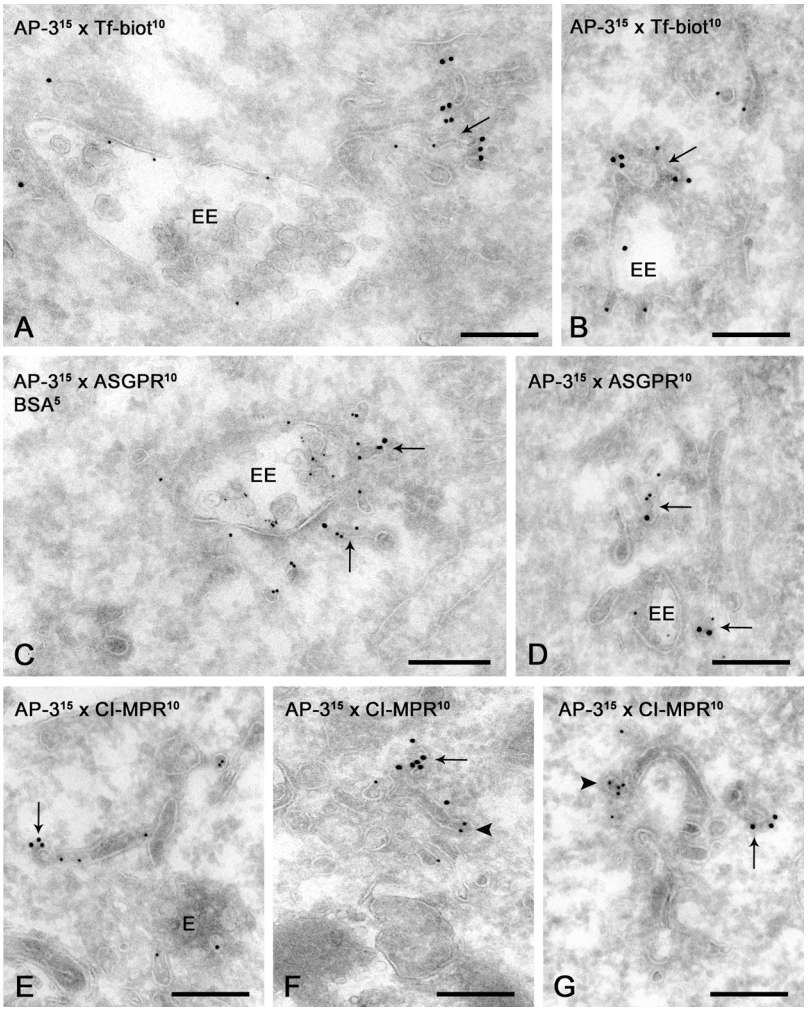

Figure 2. **Ultrathin cryosections of HepG2 cells showing the presence of AP-3 on membrane buds evolving from EE-associated tubules.** (A and B) HepG2 cells were incubated with Tf-biotin for 20 min to define early endosomes (EEs). Sections were double labeled for AP-3 (15-nm gold) and biotin (10-nm gold). AP-3 colocalizes with Tf-biotin in the recycling tubules (arrows) that emerge from the EE vacuoles. Note that AP-3 labeling is restricted to tubular endings and budding profiles on the tubules. (C) HepG2 cells were loaded for 60 min with BSA 5-nm gold, which marks the lysosomal pathway and is absent from recycling tubules. AP-3 (15-nm gold) is found on recycling tubules containing ASGPR (10-nm gold, arrows). (D) Labeling as in C, but in the absence of internalized BSA-gold. AP-3 is localized to buds that evolve from EE-associated recycling tubules containing ASGPR (arrows). (E–G) AP-3 (15-nm gold) and CI-MPR (10-nm gold). (E) Low labeling densities of CI-MPR are present in endosome (E)-associated tubules with AP-3–positive buds (arrow). (F and G) Occasionally, CI-MPR label is seen concentrated in budding profiles (arrowheads) that are not labeled for AP-3 (arrows). Bars, 200 nm.

rin-coated buds not labeled for AP-3 (Fig. 3 B). This prompted us to investigate whether different APs may associate with distinct buds of a continuous endosomal tubule. Indeed, double labeling of AP-3 and AP-1 in HepG2 cells revealed that these two coat complexes could be found on distinct buds arising from a single, continuous tubular membrane (Fig. 3 C). By triple labeling, the presence of internalized Tf-biotin was shown in the tubular membranes displaying AP-1– and AP-3–positive buds, confirming their endosomal origin (Fig. 3 D). Similar observations were

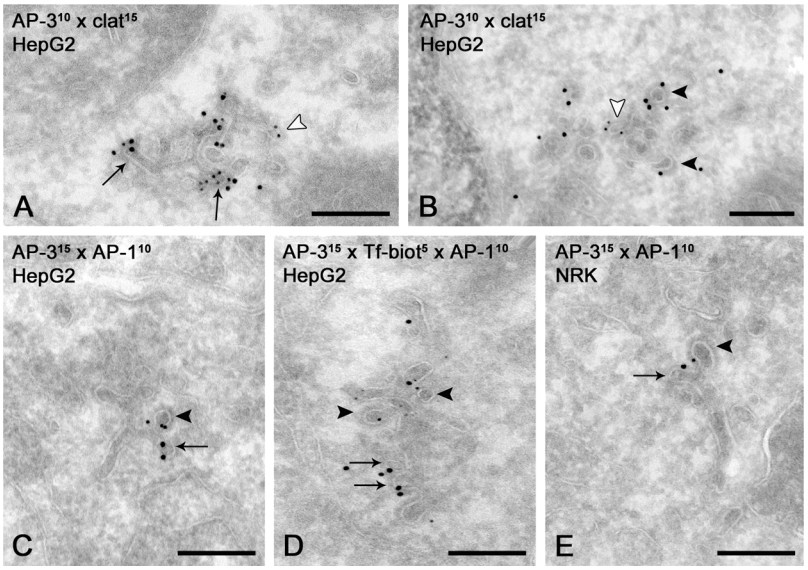

Figure 3. **AP-3–positive buds partially colocalize with clathrin, whereas AP-3 and AP-1 localize to distinct buds evolving from a single endosomal tubule.** (A and B) HepG2 cells double labeled for AP-3 (10-nm gold) and clathrin (15-nm gold). Arrows point to AP-3–positive buds that are also stained for clathrin. Open arrowheads mark membrane profiles labeled for AP-3 only. Closed arrowheads denote clathrin labeling only. (C) HepG2 cells double labeled for AP-3 (15-nm gold, arrow) and AP-1 (10-nm gold, arrowhead), showing that the two adaptor complexes are present on distinct buds of a continuous tubule. (D) Similar labeling as in A, but in addition the presence of internalized Tf-biotin (for 20 min at 37°C) is indicated by 5-nm gold, unequivocally defining the endosomal origin of this tubule. (E) NRK cells. Labeling as in A. Bars, 200 nm.

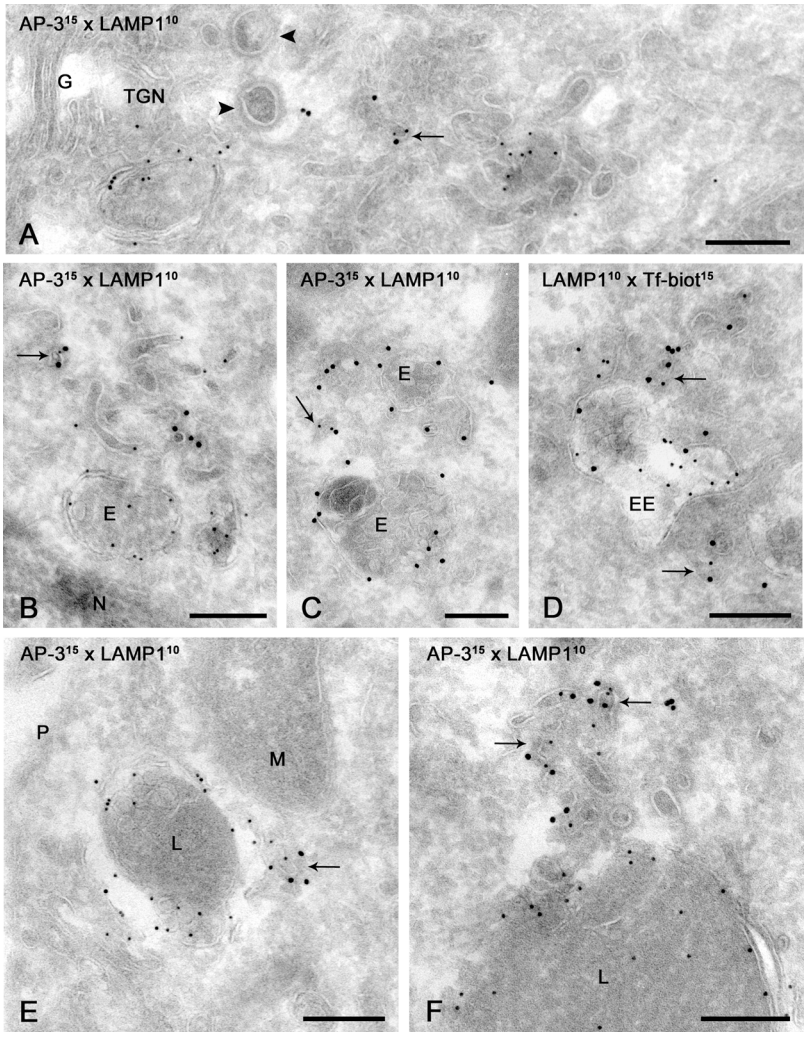

Figure 4. **LAMP-1 is concentrated in AP-3–positive budding profiles.** (A–C) Double labelings of AP-3 (15-nm gold) and LAMP-1 (10-nm gold), showing colocalization in endosome (E)-associated tubular–vesicular profiles (arrows). Low labeling densities of LAMP-1 are present in the AP-3–positive tubules. Note that in A, the LAMP-1/AP-3 positive tubule (arrow) has a smaller diameter than the typical TGN-associated clathrin-coated buds (arrowheads). (D) Colocalization of LAMP-1 (10-nm gold) and Tf-biotin internalized for 20 min (15-nm gold) unequivocally shows that LAMP-1 is present in EE-derived recycling tubules (arrows). (E and F) Double labelings of AP-3 (15-nm gold) and LAMP-1 (10-nm gold), showing that LAMP-1 is found within the AP-3–positive regions of the endosome-derived tubules (arrows). EE, early endosome; G, Golgi complex; L, lysosome; M, mitochondrion; N, nucleous; P, plasma membrane. Bars, 200 nm.

made in NRK cells (Fig. 3 E). The average size of AP-1 buds on endosomal tubules was 43 nm ($n = 37$), which is considerably smaller than AP-1 buds in the TGN (77 nm) and in the same range as the AP-3 buds (33 nm). Clathrin coats are readily visible in ultrathin cryosections (Fig. 1, A–D; Fig. 3 B; Fig. 4 A). In the AP-3 and AP-1 double-labeled cells, 46.3 ± 7.4% (average ± SEM) of AP-3 was found on clathrin-coated membranes (as defined by the presence of a dense cytosolic coat), whereas in these same cells 91 ± 8.5% of AP-1 label resided in coated membranes. Colocalization of AP-3 and AP-1 onto a single membrane bud or vesicular profile occurred to a very minor extent (<10%). We conclude from these data that AP-3 does localize with clathrin, but to a lesser extent than does AP-1, and that AP-3 and AP-1 mediate different exits from a single endosomal tubule.

LAMP-1 and LAMP-2 are concentrated in AP-3 buds on endosomal tubules

So far, our data indicate a role for AP-3 in protein traffic from the tubular recycling endosomes evolving from EEs. This was surprising because previous reports had found no effect of AP-3 deficiency on recycling proteins. Moreover, endosomal tubules are not known to be involved in the delivery of lysosomal membrane proteins to the lysosomes. To address this issue, we performed double labelings of AP-3 and LAMP-1 in HepG2 cells (Fig. 4, A–C, E, and F). The vast majority of LAMP-1 label was, as expected, found in the lysosomes (Fig. 4, E and F). LAMP-1 located in the TGN showed no colocalization with AP-3 (Fig. 4 A). Importantly, low but consistent amounts of LAMP-1 label were present in the AP-3–bearing endosomal tubules (Fig. 4, B and C). LAMP-1 colocalized with internalized Tf-biotin in EE vacuoles and in the surrounding tubules, reinforcing the notion that LAMP-1 is present in EE-associated tubules (Fig. 4 D). Finally, we performed a triple labeling between AP-3, LAMP-1, and ASGPR. LAMP-1 was found together with ASGPR in the endosome-associated tubules labeled for AP-3 (Fig. 5).

During our experiments, we noticed that the labeling for LAMP-1 was often found precisely in the AP-3–positive buds emerging from the endosomal tubules (Fig. 4, A–C, E, and F; Fig. 5, B and C). We then performed quantitative EM analysis to establish the concentrations of LAMP-1, LAMP-2, CI-MPR, and ASGPR in AP-3 budding profiles relative to that in the continuous, associated membranes lacking AP-3 (Table I; see Materials and methods for a more detailed description). Membranes in continuity with the AP-3–positive membrane buds were divided in noncoated tubular regions (Table I, column B) and AP-3–negative buds (Table I, col-

Table I. **Lysosomal membrane proteins are concentrated in AP-3–labeled regions of tubular sorting endosomes**

		Labeling density (gold/intersection)			
		(A) AP-3^{positive}	(B) AP-3^{negative} (noncoated)	(C) AP-3^{negative} (coated)	A/B
HepG2	LAMP-1	0.34 ± 0.03	0.04 ± 0.03	0.03 ± 0.02	8.5
HepG2	LAMP-2	0.36 ± 0.04	0.10 ± 0.05	0.05 ± 0.02	3.6
HepG2	CI-MPR	0.15 ± 0.03	0.15 ± 0.04	0.15 ± 0.02	1.0
HepG2	ASGPR	0.13 ± 0.03	0.14 ± 0.07	0.16 ± 0.02	0.9
Rescued *mocha*	LAMP-1	0.34 ± 0.01	0.01 ± 0.01	0.03 ± 0.03	34

Numbers represent the labeling densities ± SEM of the indicated cargo proteins in distinct regions of AP-3–positive compartments. Within AP-3–positive membrane tubules, three membrane categories were discriminated: (A) AP-3–positive membrane buds and vesicles; (B) AP-3–negative, noncoated often tubular membranes; and (C) AP-3–negative but visibly coated membrane buds. B and C were only defined when seen in continuity with A.

umn C), which amongst others will include the AP-1–coated buds and AP-3–independent concentration sites such as is shown for CI-MPR (Fig. 2, F and G). To measure the enrichment for cargo proteins in AP-3–positive buds, we therefore divided the labeling density in the AP-3–positive buds by that in the nonconcentrating, noncoated regions of the tubule (Table I, column A/B). This clearly showed that LAMP-1 and LAMP-2 are concentrated in AP-3 buds over the attached AP-3–negative membrane tubules, by factors of 8.5 and 3.6, respectively. By contrast, the ASGPR and CI-MPR are not enriched in the AP-3–positive buds. These results suggest that AP-3 plays a role in the segregation and concentration of LAMP-1 and LAMP-2 (but not CI-MPR and ASGPR) within the tubular endosomal compartment.

Loss of AP-3 leads to increased levels of recycling of LAMP-1 and CD63 back to the cell surface

From our immuno-EM experiments, we would predict that loss of AP-3 should lead to increased recycling of LAMP-1 and CD63 via the cell surface due to the decreased efficiency of lysosomal delivery from the tubular endosomes. To test this hypothesis, we decided to look at the trafficking of both LAMP-1 and CD63 in AP-3–deficient and rescued fibroblasts, using flow cytometry. Due to the lack of an antibody against mouse CD63, a *mocha* cell line was generated that expressed human CD63 at a similar level to that of endogenous LAMP-1 (Fig. S2, available at http://www.jcb.org/cgi/content/full/jcb.200311064/DC1). This cell line was then subsequently infected with either empty virus (Fig. 6 A, mock) or virus expressing the δ subunit of the AP-3 complex (Fig. 6 A, rescued). By immuno-EM, AP-3 in rescued *mocha* cells showed a similar labeling pattern as in HepG2 cells (Fig. S3); AP-3 was readily detected on endosome-associated tubules where it colocalized with LAMP-1. Quantitation of LAMP-1 labeling density over AP-3–bearing tubules revealed a marked concentration of LAMP-1 in the AP-3–positive buds (Table I). Using the *mocha* cells as negative control, the relative distribution of AP-3 in rescued *mocha* cells was established (Table II). This quantitative approach revealed low

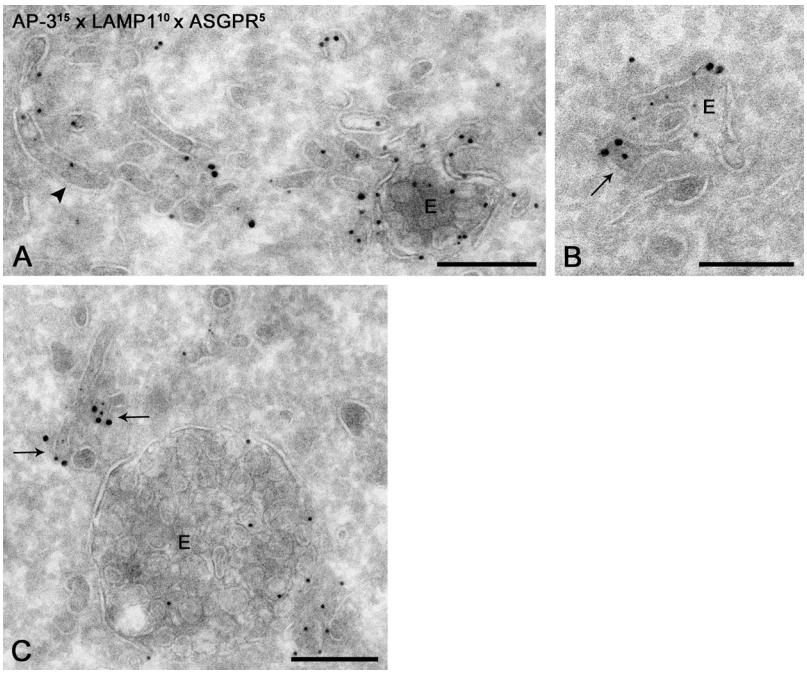

Figure 5. **LAMP-1 concentrates in AP-3–coated buds on ASGPR-positive tubular endosomes.** (A–C) HepG2 cells triple labeled for AP-3 (15-nm gold), LAMP-1 (10-nm gold), and ASGPR (5-nm gold). In A, note the extensive network of endosome (E)-associated tubules (arrowhead) that labels positive for all three proteins. In B and C, the arrows point to AP-3–positive parts of the ASGPR-labeled tubules that contain LAMP-1. Bars, 200 nm.

Table II. **Relative distribution (%) of AP-3 in rescued *mocha* cells**

TGN	Endosomal tubules/vesicles	Cytosolic tubules/vesicles	Endosomal vacuole		Undefined
			Limiting	Lumenal	
4	37	41	5	1	6

Numbers represent the percentages of total AP-3–representing gold particles that were found over the indicated compartments. The TGN was defined as membranes ≤500 nm at the trans-side of a Golgi complex. Endosomal tubules/vesicles include all membrane profiles ≤200 nm from an endosomal vacuole. All AP-3–labeled vesicular–tubular profiles not associated with a Golgi complex or endosome in the plane of the section were designated as cytosolic. The percentages were calculated after correction for background labeling in *mocha* cells, and were based on the counting of 500 ad random encountered cell profiles.

levels (4%) of staining in the TGN (defined as within 500 nm of the trans-side of a Golgi complex), whereas 43% of the label was found on the characteristic tubular membranes near endosomal vacuoles (Table II, Fig. S3). 40% of the AP-3 label was associated with tubulo-vesicular profiles that within the plain of the section were not in close vicinity of an endosomal vacuole or the Golgi complex.

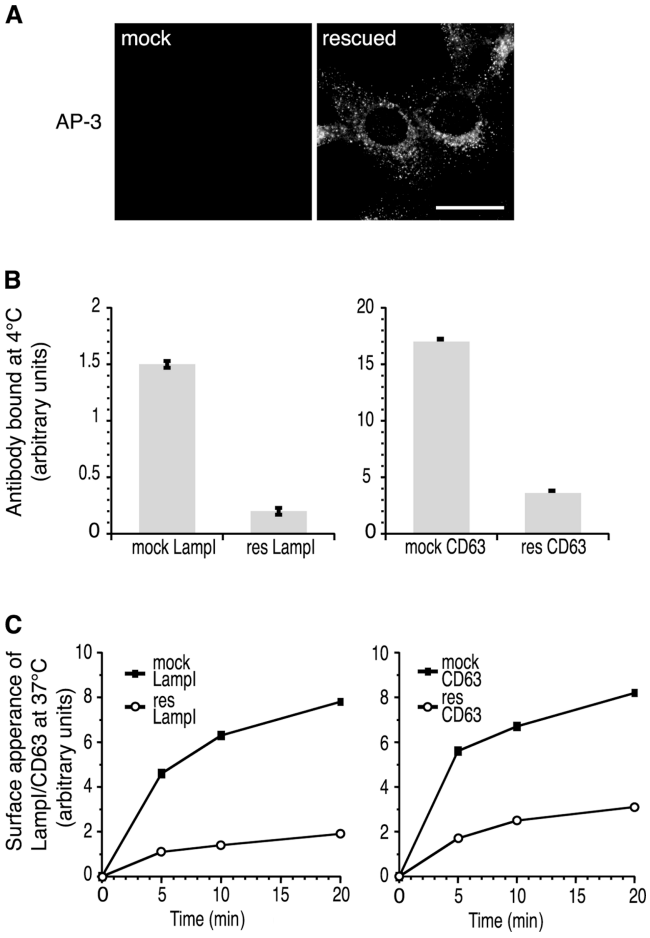

Figure 6. **AP-3 deficiency leads to increased levels of LAMP-1 and CD63 on the cell surface.** *mocha* cells expressing human CD63 were infected with either empty virus (mock) or virus expressing the δ subunit of the AP-3 complex (rescued). (A) After selection, >95% of the *mocha* cells was rescued. Bar, 30 μm. (B) Mock and rescued cells were incubated with either anti-LAMP-1 or anti-CD63 antibodies at 4°C. The steady-state levels of LAMP-1 and CD63 at the cell surface are greatly increased in AP-3–deficient cells, as determined by flow cytometry. (C) Mock and rescued cells were incubated for 20 min with either anti-LAMP-1 or anti-CD63 antibodies at 37°C. The delivery of LAMP-1 and CD63 to the cells surface is greatly decreased in rescued cells, as determined by flow cytometry. See also Fig. S3 (available at http://www.jcb.org/cgi/content/full/jcb.200311064/DC1).

Notably, we found that the levels of LAMP-1 and CD63 were greatly increased on the cell surface in mock-transfected cells (AP-3 deficient) compared with rescued *mocha* cells (approximately eight- and fivefold, respectively; Fig. 6 B). Interestingly, the level of CD63 at the cell surface is far greater than that of LAMP-1 both in mock and rescued cells (Fig. 6 B and Fig. S2). In agreement with the steady-state levels, the amount of LAMP-1 and CD63 delivered to the cell surface is also greatly increased in mock compared with rescued cells (Fig. 6 C; for triplicate experiments see Fig. S4, available at http://www.jcb.org/cgi/content/full/jcb.200311064/DC1). These data confirm previous reports showing increased trafficking of LAMP-1 and CD63 over the plasma membrane of AP-3–deficient cells (Dell'Angelica et al., 1999), but do not discriminate between proteins derived from the TGN or endosomes. To address this point, we next looked at the levels of recycling of internalized anti-TfR, anti-LAMP-1, and anti-CD63 antibodies fed to the cells in a 20-min pulse (Fig. 7). No significant difference was detected between TfR recycling in mock and rescued cells. This result was confirmed by assaying Tf recycling (unpublished data). However, in agreement with the proposed role for AP-3 on tubular endosomes, we detected a significant increase in antibody recycling for LAMP-1 and CD63 in mock compared with rescued cells (~1.8–3.3- and 1.7–2.1-fold increase, respectively; experiments were performed in triplicate and similar results were obtained and shown in Fig. S5).

Discussion

Despite significant progress in our understanding of AP-3 structure, function, and regulation, several important questions have remained unanswered: (1) the subcellular localization of AP-3; (2) the transport step of lysosomal membrane proteins that is mediated by AP-3; and (3) the physiological significance of clathrin in AP-3–dependent trafficking. In this work, we have generated an mAb against the δ subunit of AP-3 to localize the complex by immuno-EM, and have studied the trafficking of lysosomal membrane proteins in AP-3–deficient cells. Collectively, our data reveal that the AP-3 complex marks a thus far unrecognized exit site for lysosomal membrane proteins from endosome-associated tubules.

First, we set out to address to what compartment (or compartments) the AP-3 complex localizes in mammalian cells. In HepG2 cells, AP-3 was typically found on budding profiles emerging from endosomal tubules containing internalized Tf-biotin and ASGPR, two classical markers of the endosomal recycling pathway (Dautry-Varsat et al., 1983; Geuze et al., 1983; Klausner et al., 1983; Hopkins et al., 1994), and CI-MPR, which recycles between endosomes and the TGN (Kornfeld and Mellman, 1989). In addition, AP-3–bearing tubules contained the lysosomal proteins LAMP-1 and LAMP-2 and displayed distinct, small-sized AP-1–positive buds. AP-1 on endosomal tubules has been implicated in retrograde transport of MPR46 and Shiga toxin B subunit to the TGN (Mallard et al., 1998; Meyer et al., 2000), as well as recycling of internalized Tf (Mallard et al., 1998; van Dam and Stoorvogel, 2002). The presence of distinct types of recycling proteins and the association of multiple adaptor complexes suggest that from the AP-3–containing tubular endosomes, proteins are sorted to distinct destinations in the cell. Therefore, the AP-3–positive compartment is best referred to as tubular sorting endosome. A point of future interest will be to define the physical and functional boundaries between the tubular sorting endosome, vacuolar sorting endosomes, and tubular recycling endosomes.

Our quantitative analyses revealed that of the different types of cargo proteins present in the tubular sorting endosomes, only LAMP-1 and LAMP-2 were concentrated in the AP-3–positive buds and associated vesicular profiles (Table I). By contrast, ASGPR and CI-MPR were equally distributed over the AP-3–bearing and nonlabeled regions of the endosomal tubules. These findings imply that AP-3 on tubular sorting endosomes mediates an exit specific for lysosomal membrane proteins. Lysosomal membrane proteins may reach EEs via a direct pathway from the TGN or by following the constitutive secretory pathway to the cell surface and subsequent endocytosis (for review see Peters and von Figura, 1994; Hunziker and Geuze, 1996; Rouille et al., 2000). In rat hepatocytes, 45% of newly synthesized LAMP-2 and at least 25% of LAMP-1 passes through EEs before it reaches later compartments (Akasaki et al., 1995, 1996). A first possible pathway to the lysosome is then by incorporation into the intra-endosomal vesicles that form by inward budding of the limiting membrane, and this leads to the formation of multivesicular bodies (reviewed by Geuze, 1998). Sorting into intra-endosomal vesicles is an active, signal-mediated event, whereas recycling from EEs back to the cell surface can occur by default (Dunn et al., 1989; Jing et al., 1990; Mayor et al., 1993; Verges et al., 1999; Sachse et al., 2002). Lysosomal membrane proteins that are not sorted into the intra-endosomal vesicles will enter the tubular sorting endosomes. Our data suggest that from here a second, AP-3–mediated sorting step to the lysosomes originates (see Fig. 8 for a model). As suggested previously (Dell'Angelica et al., 1999; Starcevic et al., 2002), the model in Fig. 8 also accounts for the increased transport of lysosomal proteins via the plasma membrane in AP-3–deficient cells. Specifically, if AP-3 deficiency impairs transport from tubular sorting endosomes to lysosomes, it will lead to an increased incorporation of lysosomal membrane proteins into the default recycling pathway to the plasma membrane. Indeed, this was what we observed when we compared the level of recycling of endocytosed LAMP-1 and CD63 to the plasma membrane in AP-3–deficient and rescued fibroblasts, providing additional strong evidence that AP-3 acts on an endosomal compartment. Consistent with previous papers (Le Borgne et al., 1998; Dell'Angelica et al., 1999), recycling of the TfR was unaffected in the AP-3–deficient cells.

We do not suggest that the AP-3 pathway is the only route to lysosomes. At least a portion of lysosomal membrane proteins will reach the lysosomes via the intra-endosomal vesicles (Geuze, 1998). In addition, although we do not find a role for AP-3 in transport from the TGN to late endosomes or lysosomes, there is compelling evidence that

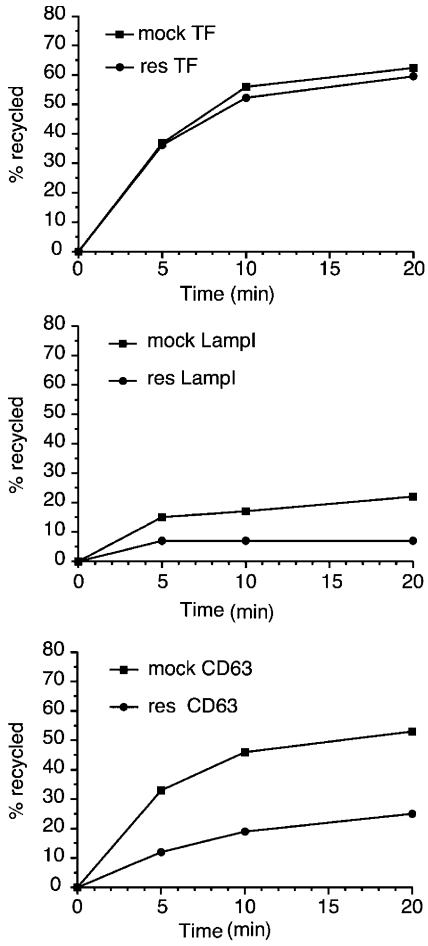

Figure 7. **AP-3 deficiency leads to the increased recycling of lysosomal membrane proteins via the cell surface.** Mock and rescued cells were allowed to internalize antibodies against LAMP-1, CD63, and TfR for 20 min at 37°C. The cells were washed and the amount of recycling was determined by incubating the cells for various amounts of time at 37°C in the presence of quenching antibody (anti-Alexa® 488). The cells were then analyzed by flow cytometry. The degree of recycling of LAMP-1 and CD63 is greatly enhanced in AP-3–deficient cells (mock); however, recycling of the TfR is unaffected. See also Fig. S4 (available at http://www.jcb.org/cgi/content/full/jcb.200311064/DC1).

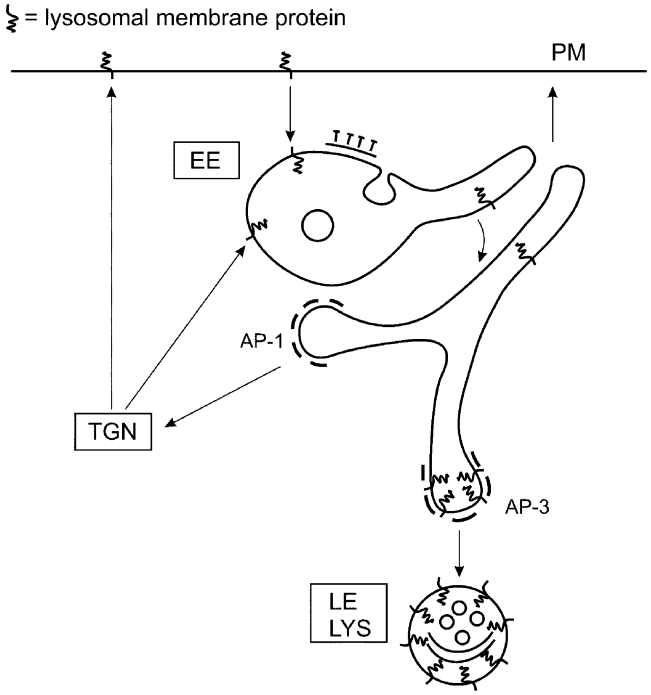

Figure 8. **Proposed role for AP-3 in the trafficking of lysosomal membrane proteins.** Lysosomal membrane proteins reach EE vacuoles (or sorting endosomes) directly from the TGN or from an indirect pathway via the plasma membrane. Proteins that are not incorporated into the internal endosomal vesicles will by default enter the tubular extensions that emerge from the endosomal vacuole. The default pathway from the tubular endosomes is to the plasma membrane, but there is also an AP-1– and AP-3–mediated exit. The AP-3–containing membranes selectively concentrate lysosomal membrane proteins rather than proteins destined for TGN or plasma membrane, thus we propose they mediate transport to late endosomes/lysosomes. In this model, if AP-3 function were impaired, it would lead to an increased incorporation of lysosomal membrane proteins in the default recycling pathway, resulting in increased passage of lysosomal membrane proteins over the plasma membrane. E, early endosome; LE, late endosome; LYS, lysosome; PM, plasma membrane.

such a direct pathway does exist, possibly using another coat complex (Rouille et al., 2000). An indication that there are indeed many routes to the lysosome is highlighted in cells that are deficient in both AP-1 and AP-3 because lysosomal proteins still localize to the lysosomes (Reusch et al., 2002). The efficiency by which a pathway is taken may differ between cells and may depend on the expression levels (Harter and Mellman, 1992). In this respect, an interesting additional conclusion from the internalization and recycling assays in the rescued *mocha* cells (Fig. 6 and Fig. 7) is that LAMP-1 and CD63 appear to use distinct pathways for lysosomal delivery with different efficiencies, with more CD63 trafficking over the plasma membrane. Moreover, our assays showed that also in rescued *mocha* cells, LAMP-1 and CD63 recycle from endosomes to the plasma membrane, as was previously suggested for LAMP-2 (Akasaki et al., 1993) and avian LAMP-1 (Lippincott-Schwartz and Fambrough, 1987). These observations suggest that lysosomal membrane proteins may require several passages through EEs before they are sorted to the lysosomes.

A role for AP-3 in lysosomal membrane protein traffic from tubular sorting endosomes is in agreement with previous immuno-EM data in PC12 and A431 cells (Dell'Angelica et al., 1998), and with the recent observation that in AP-3–deficient cytotoxic T-lymphocytes, tubular endosomes elongate (Clark et al., 2003). Our observations are in contrast to a previous immuno-EM experiment in NRK cells by Simpson et al. (1996), showing that AP-3 labeling is mainly associated with the TGN. However, some of the localization experiments of Simpson et al. (1996) were done in the presence of GTPγS, which can lead to the mislocalization of coat complexes (Seaman et al., 1993). By in vitro recruitment experiments in *mocha* cells in the presence of GTPγS, it was found that the AP-3 complex indeed distributes to a more perinuclear location than normal (unpublished data). We defined the TGN as the membrane network within ~500 nm of the trans-side of the Golgi stack (Geuze et al., 1985). Our quantitations in rescued *mocha* cells revealed that 4% of total AP-3 label was found on membranes that by this definition were classified as TGN. 41% of the AP-3 label was found on tubulo-vesicular membranes associated with endosomes, whereas 40% of AP-3 label was not clearly associated with either endosomes or TGN (indicated as cytoplasmic). The majority of the cytoplasmic membranes is probably of endosomal origin, but we cannot exclude that they include peripheral TGN profiles as well (Puertollano et al., 2003; Waguri et al., 2003). Therefore, it remains possible that AP-3 does play a minor role in the trafficking of cargo molecules from the TGN, as was also suggested by others (Nishimura et al., 2002; Rous et al., 2002).

Another issue we addressed was the potential interaction of the AP-3 complex with clathrin. The association of AP-3 with clathrin has been shown previously (Dell'Angelica et al., 1998), but we provide here the first quantitative analysis in direct comparison with a well-known clathrin-binding adaptor, AP-1. We found in HepG2 cells 46% of AP-3–positive membranes, and 91% of AP-1–positive membranes were coated for clathrin as well. A previous work in neuroendocrine PC12 cells revealed that 65% of the AP-3–positive membranes labeled for clathrin (Dell'Angelica et al., 1998), which is possibly explained by the fact that in these cells, AP-3 is involved in clathrin-dependent formation of synaptic vesicles from endosomes (Faundez et al., 1998). Together, the data in PC12 and HepG2 cells indicate that AP-3 uses clathrin in vivo, but that at steady state its association with clathrin is significantly lower than that of AP-1. Possibly, the interaction between AP-3 and clathrin is weaker than that found with the other adaptor complexes. This would also explain why the AP-3 complex is not present in clathrin-coated vesicle preparations and why clathrin is not readily immunoprecipitated with antibodies against AP-3 (Simpson et al., 1996; unpublished data). Alternatively or additionally, the assembly of an AP-3 clathrin coat may be a relatively slow process, resulting in lower steady-state levels of association. A third possible explanation is that clathrin might play a facilitating rather than obligatory role. Clearly, further analyses are required to distinguish between these possibilities.

Materials and methods

Antibody reagents

Mouse mAbs against the AP-3 δ subunit were generated by immunizing female BALB/c mice with a GST fusion protein corresponding to the hinge domain of the δ subunit (aa 608–800 of human δ-adaptin). Fusion of the spleen cells with myeloma cells and screening of the resulting antibodies was performed as described by Bock et al. (1997). Clones that yielded an immunofluorescence pattern identical to that of an anti-δ polyclonal (Simpson et al., 1997; a gift from Dr. M.S. Robinson, University of Cambridge, Cambridge, UK) were further characterized by immuno-EM. The clone SA4 gave the most intense labeling, so it was used for all the immuno-EM experiments performed in this paper. The SA4 cell line and resultant antibodies are available from the Developmental Studies Hybridoma Bank (University of Iowa, Iowa City, IA). The following polyclonal antibodies were generously donated to us: anti-AP-1 (Dr. M. Robinson, University of Cambridge, Cambridge, UK); antibody 931B against human LAMP-1 and antibody 932.1 against human LAMP-2 (Dr. M. Fukuda, La Jolla Cancer Research Foundation, La Jolla, CA); anti–mouse lgp120/LAMP-1 (Dr. I. Mellman, Yale University, New Haven, CT); anti-CI-MPR (Dr. K. von Figura, University of Göttingen, Göttingen, Germany); antibody K1 against the ASGPR (Dr. A. Schwartz, Washington University, St. Louis, MO); and anti-clathrin (Dr. S. Corvera, University of Massachusetts Medical School, Worcester, MA). Anti-biotin 100-4198 was obtained from Rockland Immunochemicals. To compare the degree of colocalization of AP-3 and clathrin with that of AP-1 and clathrin, an mAb from Dr. E. Ungewickell (Medical University Hannover, Hannover, Germany) was used instead of the polyclonal anti-AP-1. As a bridging step between mouse mAbs and protein A–gold, we used rabbit anti–mouse (DakoCytomation). The hybridoma cell lines 1D4B (rat anti–mouse LAMP-1; Hughes and August, 1981) and H5C6 (mouse anti–human CD63) were obtained from the Developmental Studies Hybridoma Bank, developed under the auspice of the National Institute of Child Health and Human Development and maintained by the University of Iowa (Department of Biological Sciences, Iowa City, IA). The cell line TIB219 (rat anti–mouse TfR; Lesley et al., 1984) was obtained from the American Type Culture Collection. All three antibodies were purified from the culture media using an anti–rat or anti–mouse affinity column, acid eluted, and conjugated to Alexa Fluor® 488 or 594 using a protein-labeling kit according to the manufacturer's instructions (Molecular Probes, Inc.).

Flow cytometry

A quantitative assay for AP-3–dependent sorting was used as described by Peden et al. (2002), with the modifications listed below. Cells were trypsinized, washed in complete medium, and incubated with Alexa® 488–conjugated anti-LAMP-1 and anti-CD63 antibodies (2 μg/ml) for 30 min at 4°C. After shifting to 37°C for various times, the antibody binding was stopped by pelleting the cells and resuspending them in 3% formaldehyde. To determine the amount of recycling of LAMP-1, CD63, and TfR, cells were allowed to internalize labeled antibodies for 20 min, after which excess antibodies were washed away with ice-cold DME. The cells were then incubated with 24 μg/ml quenching antibody (anti-Alexa® 488; Molecular Probes, Inc.) in DME at 37°C for various times. To ensure complete quenching, the cells were placed on ice for 30 min before being fixed in 3% formaldehyde. The cells were analyzed using a flow cytometer (Epics-Xl; Beckman Coulter).

Retroviral infections

The AP-3 δ-subunit–deficient *mocha* cell line (CRL-2709; American Type Culture Collection), previously described by Peden et al. (2002), was infected with virus expressing human CD63, followed by infection with the wild-type δ subunit of the AP-3 complex or empty virus as described by Swift et al. (1999). The virus used was a version of pBMN modified such that the hygromycin selectable marker was expressed on the same transcript as the δ or CD63 messages. Infected cells were selected in 200 μg/ml hygromycin B.

Internalization of Tf-biotin and BSA-gold

Tf-biotin was obtained from Sigma-Aldrich and was iron saturated as described previously (Stoorvogel et al., 1987). HepG2 cells cultured in 6-cm-diam dishes were preincubated in MEM plus 0.1% BSA in a CO_2 incubator at 37°C, and then 20 μg/ml Tf-biotin was added and allowed to internalize for 20 min. Cells were rinsed twice with MEM containing 0.1% BSA at 4°C and fixed overnight in a final concentration of 4% formaldehyde in 0.1 M phosphate buffer, pH 7.4. BSA conjugated to 5 nm colloidal gold (final OD of 5 at 520 nm) after overnight dialysis with serum-free media was similarly used to mark the endocytic pathway, except the internalization was for 60 min in 1.5 ml MEM containing 1% FCS and 100 μl BSA 5-nm gold.

Immuno-EM

Cells were fixed by adding 4% freshly prepared formaldehyde in 0.1 M phosphate buffer, pH 7.4, to an equal volume of culture medium for 10 min, followed by post-fixation in 4% formaldehyde without medium, and were stored at 4°C. Glutaraldehyde was found to strongly reduce the AP-3 labeling. Processing of cells for ultrathin cryosectioning and immunolabeling according to the protein A–gold method was done as described previously (Slot et al., 1991; Liou et al., 1996).

To measure the diameter of AP-3– and AP-1–labeled budding profiles, pictures of positively labeled membranes were randomly taken at a magnification of 30,000 in the EM and used at an end magnification of 81,000. The diameter of a labeled bud was measured with a ruler, after which the data were recalculated to nanometers. For these countings, we did not include vesicular profiles nor the long AP-1/clathrin stretches found on the TGN. We focused on buds clearly connected to TGN or endosomes.

To measure the degree of colocalization of AP-3 and AP-1 with clathrin, HepG2 cells were double labeled for AP-3 (15-nm gold) and AP-1 (10-nm gold). By moving randomly through the grid, for each AP-3– or AP-1–representing gold particle it was established whether it was present on a membrane bearing a visible clathrin coat. In total, 380 and 341 gold particles were counted for AP-3 and AP-1, respectively, in three independent experiments.

The labeling densities of CI-MPR, ASGPR, LAMP-1, and LAMP-2 were established in series of double-labeling experiments in which AP-3 was always used in the first step. AP-3–positive membranes were selected in the EM and photographed only when they were also positive for the marker protein under analysis. Per marker protein, at least 50 pictures were taken at a magnification of 30,000 and were analyzed at an end magnification of 81,000. The pictures were overlaid with a transparent 5-mm spaced line lattice. The number of gold particles present on AP-3–positive and AP-3–negative regions of the compartments were counted, as well as the number of intersections of the distinct membrane domains with the 5-mm line lattice overlay, to give a measure of membrane length (Weibel, 1979). The labeling density was then expressed as number of gold particles per intersection, which reflects the concentration of a given protein in a membrane domain.

The relative distribution of AP-3 in rescued *mocha* cells was assessed by analyzing 500 ad random sampled cell profiles from two distinct grids. All gold particles that were no further than 25 nm from a membrane were ascribed to the compartment on which they were found. This resulted in a total of 555 gold particles over the relevant intracellular compartments. A similar analysis in *mocha* cells (prepared and labeled in the same experiment as the rescued *mochas*) yielded 74 gold particles, representing nonspecific background. After subtracting the background label over the distinct compartments from the specific label, the percentage of total label over a given compartment in rescued *mocha* cells was calculated (Table II). All tubulo-vesicular membranes within 200 nm from an endosomal vacuole were designated as being endosome associated, whereas membranes within 500 nm of the trans-side of a Golgi complex were designated TGN. Tubulo-vesicular membranes that in the plane of the section were not associated with Golgi or endosomes were designated as cytoplasmic. All pictures were taken on a transmission electron microscope (model 1010; JEOL USA, Inc.).

Immunofluorescence

Cells were cultured on multiwell slides (ICN Biomedicals), fixed for 15 min with 3% PFA in PBS, quenched for 10 min with 0.1 M glycine in PBS, permeabilized with 0.4% saponin in PBS for 10 min, and were then stained with the primary antibody for 30 min. After incubation with secondary antibody conjugated to Alexa® 488 or 594 for 20 min, coverslips were mounted onto the cells with Vectashield® (Vector Laboratories). Images were acquired using a microscope (Axiovert 200; Carl Zeiss MicroImaging, Inc.) fitted with a Plan-Apochromat 1.4 NA 63× objective, a camera (AxioCam; Carl Zeiss MicroImaging, Inc.), and a Quad pass filter set (Chroma Technology Corp.), all controlled by AxioVison 3.1 software (Carl Zeiss MicroImaging, Inc.). The brightness and contrast of acquired images was adjusted using Adobe Photoshop® v6.0.

Online supplemental material

Fig. S1 shows the characterization of mAb SA4 against the δ subunit of AP-3 that was used in this work. Fig. S2 shows the fluorescence staining of LAMP-1 and CD63 in mock-transfected and rescued *mocha* cells. Fig. S3 shows the colocalization of AP-3 and LAMP-1 in endosomal tubules of res-

cued *mocha* cells. Fig. S4 and Fig. S5 show the triplicates of the antibody binding and recycling assays described in Fig. 6 and Fig. 7, respectively. Online supplemental material available at http://www.jcb.org/cgi/content/full/jcb.200311064/DC1.

We thank Martin Sachse for assistance with the BSA-gold and Tf-biotin uptake experiments; Rene Scriwanek and Marc van Peski for the preparation of the electron micrographs; members of the Scheller and Klumperman labs for help and advice; S.J. Scales and H. Geuze for stimulating discussions; M. Robinson for numerous reagents and helpful discussions; M. Fukuda, K. von Figura, A. Schwartz, S. Corvera, E. Ungewickell, and I. Mellman for their gifts of antibodies; Kurt Schroder for the purification of antibodies; and Peter Schow for advice on flow cytometry.

Initially, A.A. Peden was supported by a grant from the Wellcome trust.

Submitted: 18 November 2003
Accepted: 13 February 2004

References

Akasaki, K., M. Fukuzawa, H. Kinoshita, K. Furuno, and H. Tsuji. 1993. Cycling of two endogenous lysosomal membrane proteins, lamp-2 and acid phosphatase, between the cell surface and lysosomes in cultured rat hepatocytes. *J. Biochem.* (*Tokyo*). 114:598–604.

Akasaki, K., A. Michihara, K. Mibuka, Y. Fujiwara, and H. Tsuji. 1995. Biosynthetic transport of a major lysosomal membrane glycoprotein, lamp-1: convergence of biosynthetic and endocytic pathways occurs at three distinctive points. *Exp. Cell Res.* 220:464–473.

Akasaki, K., A. Michihara, Y. Fujiwara, K. Mibuka, and H. Tsuji. 1996. Biosynthetic transport of a major lysosome-associated membrane glycoprotein 2, lamp-2: a significant fraction of newly synthesized lamp-2 is delivered to lysosomes by way of early endosomes. *J. Biochem.* (*Tokyo*). 120:1088–1094.

Bock, J.B., J. Klumperman, S. Davanger, and R.H. Scheller. 1997. Syntaxin 6 functions in trans-Golgi network vesicle trafficking. *Mol. Biol. Cell.* 8:1261–1271.

Clark, R.H., J.C. Stinchcombe, A. Day, E. Blott, S. Booth, G. Bossi, T. Hamblin, E.G. Davies, and G.M. Griffiths. 2003. Adaptor protein 3-dependent microtubule-mediated movement of lytic granules to the immunological synapse. *Nat. Immunol.* 4:1111–1120.

Cowles, C.R., G. Odorizzi, G.S. Payne, and S.D. Emr. 1997. The AP-3 adaptor complex is essential for cargo-selective transport to the yeast vacuole. *Cell.* 91:109–118.

Dautry-Varsat, A., A. Ciechanover, and H.F. Lodish. 1983. pH and the recycling of transferrin during receptor-mediated endocytosis. *Proc. Natl. Acad. Sci. USA.* 80:2258–2262.

Dell'Angelica, E.C., H. Ohno, C.E. Ooi, E. Rabinovich, K.W. Roche, and J.S. Bonifacino. 1997. AP-3: an adaptor-like protein complex with ubiquitous expression. *EMBO J.* 16:917–928.

Dell'Angelica, E.C., J. Klumperman, W. Stoorvogel, and J.S. Bonifacino. 1998. Association of the AP-3 adaptor complex with clathrin. *Science.* 280:431–434.

Dell'Angelica, E.C., V. Shotelersuk, R.C. Aguilar, W.A. Gahl, and J.S. Bonifacino. 1999. Altered trafficking of lysosomal proteins in Hermansky-Pudlak syndrome due to mutations in the β3A-subunit of the AP-3 adaptor. *Mol. Cell.* 3:11–21.

Doray, B., P. Ghosh, J. Griffith, H.J. Geuze, and S. Kornfeld. 2002. Cooperation of GGAs and AP-1 in packaging MPRs at the trans-Golgi network. *Science.* 297:1700–1703.

Drake, M.T., Y. Zhu, and S. Kornfeld. 2000. The assembly of AP-3 adaptor complex-containing clathrin-coated vesicles on synthetic liposomes. *Mol. Biol. Cell.* 11:3723–3736.

Dunn, K.W., T.E. McGraw, and F.R. Maxfield. 1989. Iterative fractionation of recycling receptors from lysosomally destined ligands in an early sorting endosome. *J. Cell Biol.* 109:3303–3314.

Faundez, V., J.T. Horng, and R.B. Kelly. 1998. A function for the AP3 coat complex in synaptic vesicle formation from endosomes. *Cell.* 93:423–432.

Geuze, H.J. 1998. The role of endosomes and lysosomes in MHC class II functioning. *Immunol. Today.* 19:282–287.

Geuze, H.J., J.W. Slot, G.J. Strous, H.F. Lodish, and A.L. Schwartz. 1983. Intracellular site of asialoglycoprotein receptor-ligand uncoupling: double-label immunoelectron microscopy during receptor-mediated endocytosis. *Cell.* 32:277–287.

Geuze, H.J., J.W. Slot, G.J. Strous, A. Hasilik, and K. von Figura. 1985. Possible pathways for lysosomal enzyme delivery. *J. Cell Biol.* 101:2253–2262.

Griffiths, G., R. Back, and M. Marsh. 1989. A quantitative analysis of the endocytic pathway in baby hamster kidney cells. *J. Cell Biol.* 109:2703–2720.

Harter, C., and I. Mellman. 1992. Transport of the lysosomal membrane glycoprotein lgp120 (lgpA) to lysosomes does not require appearance on the plasma membrane. *J. Cell Biol.* 117:311–325.

Heuser, J.E., and J. Keen. 1988. Deep-etch visualization of proteins involved in clathrin assembly. *J. Cell Biol.* 107:877–886.

Hopkins, C.R., A. Gibson, M. Shipman, D.K. Strickland, and I.S. Trowbridge. 1994. In migrating fibroblasts, recycling receptors are concentrated in narrow tubules in the pericentriolar area, and then routed to the plasma membrane of the leading lamella. *J. Cell Biol.* 125:1265–1274.

Hughes, E.N., and J.T. August. 1981. Characterization of plasma membrane proteins identified by monoclonal antibodies. *J. Biol. Chem.* 256:664–671.

Hunziker, W., and H.J. Geuze. 1996. Intracellular trafficking of lysosomal membrane proteins. *Bioessays.* 18:379–389.

Jing, S.Q., T. Spencer, K. Miller, C. Hopkins, and I.S. Trowbridge. 1990. Role of the human transferrin receptor cytoplasmic domain in endocytosis: localization of a specific signal sequence for internalization. *J. Cell Biol.* 110:283–294.

Klausner, R.D., G. Ashwell, J. van Renswoude, J.B. Harford, and K.R. Bridges. 1983. Binding of apotransferrin to K562 cells: explanation of the transferrin cycle. *Proc. Natl. Acad. Sci. USA.* 80:2263–2266.

Klumperman, J., A. Hille, T. Veenendaal, V. Oorschot, W. Stoorvogel, K. von Figura, and H.J. Geuze. 1993. Differences in the endosomal distributions of the two mannose 6-phosphate receptors. *J. Cell Biol.* 121:997–1010.

Kornfeld, S., and I. Mellman. 1989. The biogenesis of lysosomes. *Annu. Rev. Cell Biol.* 5:483–525.

Le Borgne, R., A. Alconada, U. Bauer, and B. Hoflack. 1998. The mammalian AP-3 adaptor-like complex mediates the intracellular transport of lysosomal membrane glycoproteins. *J. Biol. Chem.* 273:29451–29461.

Lesley, J., R. Hyman, R. Schulte, and J. Trotter. 1984. Expression of transferrin receptor on murine hematopoietic progenitors. *Cell. Immunol.* 83:14–25.

Liou, W., H.J. Geuze, and J.W. Slot. 1996. Improving structural integrity of cryosections for immunogold labeling. *Histochem. Cell Biol.* 106:41–58.

Lippincott-Schwartz, J., and D.M. Fambrough. 1987. Cycling of the integral membrane glycoprotein, LEP100, between plasma membrane and lysosomes: kinetic and morphological analysis. *Cell.* 49:669–677.

Mallard, F., C. Antony, D. Tenza, J. Salamero, B. Goud, and L. Johannes. 1998. Direct pathway from early/recycling endosomes to the Golgi apparatus revealed through the study of shiga toxin B-fragment transport. *J. Cell Biol.* 143:973–990.

Marsh, M., G. Griffiths, G.E. Dean, I. Mellman, and A. Helenius. 1986. Three-dimensional structure of endosomes in BHK-21 cells. *Proc. Natl. Acad. Sci. USA.* 83:2899–2903.

Mayor, S., J.F. Presley, and F.R. Maxfield. 1993. Sorting of membrane components from endosomes and subsequent recycling to the cell surface occurs by a bulk flow process. *J. Cell Biol.* 121:1257–1269.

Meyer, C., D. Zizioli, S. Lausmann, E.L. Eskelinen, J. Hamann, P. Saftig, K. von Figura, and P. Schu. 2000. μ1A adaptin-deficient mice: lethality, loss of AP-1 binding and rerouting of mannose 6-phosphate receptors. *EMBO J.* 19:2193–2203.

Nishimura, N., H. Plutner, K. Hahn, and W.E. Balch. 2002. The δ subunit of AP-3 is required for efficient transport of VSV-G from the trans-Golgi network to the cell surface. *Proc. Natl. Acad. Sci. USA.* 99:6755–6760.

Odorizzi, G., C.R. Cowles, and S.D. Emr. 1998. The AP-3 complex: a coat of many colours. *Trends Cell Biol.* 8:282–288.

Peden, A.A., R.E. Rudge, W.W. Lui, and M.S. Robinson. 2002. Assembly and function of AP-3 complexes in cells expressing mutant-subunits. *J. Cell Biol.* 156:327–336.

Peters, C., and K. von Figura. 1994. Biogenesis of lysosomal membranes. *FEBS Lett.* 346:108–114.

Puertollano, R., N.N. van der Wel, L.E. Greene, E. Eisenberg, P.J. Peters, and J.S. Bonifacino. 2003. Morphology and dynamics of clathrin/GGA1-coated carriers budding from the trans-Golgi network. *Mol. Biol. Cell.* 14:1545–1557.

Reusch, U., O. Bernhard, U. Koszinowski, and P. Schu. 2002. AP-1A and AP-3A lysosomal sorting functions. *Traffic.* 3:752–761.

Robinson, M.S., and J.S. Bonifacino. 2001. Adaptor-related proteins. *Curr. Opin. Cell Biol.* 13:444–453.

Rouille, Y., W. Rohn, and B. Hoflack. 2000. Targeting of lysosomal proteins. *Semin. Cell Dev. Biol.* 11:165–171.

Rous, B.A., B.J. Reaves, G. Ihrke, J.A. Briggs, S.R. Gray, D.J. Stephens, G.

Banting, and J.P. Luzio. 2002. Role of adaptor complex AP-3 in targeting wild-type and mutated CD63 to lysosomes. *Mol. Biol. Cell.* 13:1071–1082.

Sachse, M., S. Urbe, V. Oorschot, G.J. Strous, and J. Klumperman. 2002. Bilayered clathrin coats on endosomal vacuoles are involved in protein sorting toward lysosomes. *Mol. Biol. Cell.* 13:1313–1328.

Seaman, M.N., C.L. Ball, and M.S. Robinson. 1993. Targeting and mistargeting of plasma membrane adaptors in vitro. *J. Cell Biol.* 123:1093–1105.

Simpson, F., N.A. Bright, M.A. West, L.S. Newman, R.B. Darnell, and M.S. Robinson. 1996. A novel adaptor-related protein complex. *J. Cell Biol.* 133:749–760.

Simpson, F., A.A. Peden, L. Christopoulou, and M.S. Robinson. 1997. Characterization of the adaptor-related protein complex, AP-3. *J. Cell Biol.* 137:835–845.

Slot, J.W., H.J. Geuze, S. Gigengack, G.E. Lienhard, and D.E. James. 1991. Immuno-localization of the insulin regulatable glucose transporter in brown adipose tissue of the rat. *J. Cell Biol.* 113:123–135.

Starcevic, M., R. Nazarian, and E.C. Dell'Angelica. 2002. The molecular machinery for the biogenesis of lysosome-related organelles: lessons from Hermansky-Pudlak syndrome. *Semin. Cell Dev. Biol.* 13:271–278.

Stepp, J.D., K. Huang, and S.K. Lemmon. 1997. The yeast adaptor protein complex, AP-3, is essential for the efficient delivery of alkaline phosphatase by the alternate pathway to the vacuole. *J. Cell Biol.* 139:1761–1774.

Stoorvogel, W., H.J. Geuze, and G.J. Strous. 1987. Sorting of endocytosed transferrin and asialoglycoprotein occurs immediately after internalization in HepG2 cells. *J. Cell Biol.* 104:1261–1268.

Sugita, M., X. Cao, G.F. Watts, R.A. Rogers, J.S. Bonifacino, and M.B. Brenner. 2002. Failure of trafficking and antigen presentation by CD1 in AP-3-deficient cells. *Immunity.* 16:697–706.

Swift, S., J.B. Lorens, P. Achacoso, and G.P. Nolan. 1999. Rapid production of retroviruses for efficient gene delivery to mammalian cells using 293T cell-based systems. *In* Current Protocols in Immunology. J.E. Coligan, A.M. Kruisbeek, D.H. Margulies, E.M. Shevach, and W. Strober, editors. John Wiley & Sons Inc., New York. Suppl. 31.

ter Haar, E., S.C. Harrison, and T. Kirchhausen. 2000. Peptide-in-groove interactions link target proteins to the β-propeller of clathrin. *Proc. Natl. Acad. Sci. USA.* 97:1096–1100.

van Dam, E.M., and W. Stoorvogel. 2002. Dynamin-dependent transferrin receptor recycling by endosome-derived clathrin-coated vesicles. *Mol. Biol. Cell.* 13:169–182.

Verges, M., R.J. Havel, and K.E. Mostov. 1999. A tubular endosomal fraction from rat liver: biochemical evidence of receptor sorting by default. *Proc. Natl. Acad. Sci. USA.* 96:10146–10151.

Vowels, J.J., and G.S. Payne. 1998. A dileucine-like sorting signal directs transport into an AP-3-dependent, clathrin-independent pathway to the yeast vacuole. *EMBO J.* 17:2482–2493.

Waguri, S., F. Dewitte, R. Le Borgne, Y. Rouille, Y. Uchiyama, J.F. Dubremetz, and B. Hoflack. 2003. Visualization of TGN to endosome trafficking through fluorescently labeled MPR and AP-1 in living cells. *Mol. Biol. Cell.* 14:142–155.

Weibel, E.R. 1979. Stereological Methods: Practical Methods for Biological Morphometry. Vol. 1. Academic Press, London/New York. 415 pp.

Wettey, F.R., S.F. Hawkins, A. Stewart, J.P. Luzio, J.C. Howard, and A.P. Jackson. 2002. Controlled elimination of clathrin heavy-chain expression in DT40 lymphocytes. *Science.* 297:1521–1525.